Effects of Hydrostatic Pressure on the Kinetics Reveal a Volume Increase during the Bacteriorhodopsin Photocycle†

György Váró‡ and Janos K. Lanyi*

Department of Physiology & Biophysics, University of California, Irvine, California 92717

Received June 9, 1995; Revised Manuscript Received July 18, 1995⊗

ABSTRACT: A protein structural change in the photocycle of the proton pump, bacteriorhodopsin, detected earlier in the M photointermediate by diffraction, consists mainly of changes at the cytoplasmic surface that include an outward tilt of the cytoplasmic end of helix F. Such a conformational rearrangement would result in greater exposure of the interhelical cavity to the medium, increased binding of water, and thus an increase in volume. In order to correlate the structural change with the kinetics of the photoreaction cycle, we measured the effects of hydrostatic pressure between 1 bar and 1 kbar on the rate constants of the photocycles of wild type bacteriorhodopsin and the D96N mutant. Combining the results provided all of the activation volumes and, therefore, the changes of volume in the various states after the K photointermediate is formed. There is an approximately 32 mL/mol volume increase after deprotonation of the retinal Schiff base to the extracellular side, during the $M_1 \rightarrow M_2$ reaction, that is not reversed until well after its reprotonation from the cytoplasmic side. The magnitude of this volume increase is about as predicted by the increase of the lattice constant in the M state. It occurs in the photocycle at the proposed reprotonation switch, supporting the idea that this conformation change is what alters the accessibility of the Schiff base from one membrane side to the other. Additionally, we observe a large positive (approximately 50 mL/mol) activation volume for proton exchange between D96 and the Schiff base of the wild type protein. This is consistent with a requirement for increased hydration of the protein near D96 for the proton exchange to occur, as suggested earlier from the specific inhibition of this step by osmotically active solutes.

Bacteriorhodopsin is a small retinal-protein in the cytoplasmic membrane of halobacteria [reviewed in Mathies et al. (1991), Tittor (1991), Ebrey (1993), Krebs & Gobind Khorana (1993), Lanyi (1993)]. The light-induced transient all-*trans* to 13-*cis* isomerization of the retinal chromophore sets off a series of proton transfers inside the protein and at the two membrane surfaces that result in the net translocation of a proton. The details of the thermal reactions during this process (the "photocycle") have been intensively studied because the conceptual and experimental simplicity of this system had raised the hope that it will be easier to understand bacteriorhodopsin than other ion pumps, and the insights gained will lead to insights into ion pumps in general.

The photocycle has been described as the sequence

$$BR \xrightarrow{h\nu} K \leftrightarrow L \leftrightarrow M_1 \rightarrow M_2 \leftrightarrow N \leftrightarrow O \rightarrow Br$$

(Ames & Mathies, 1990; Gerwert et al., 1990; Váró & Lanyi, 1991b; Souvignier & Gerwert, 1992; Lozier et al., 1992), where the lettered states[1] differ in the configurational state of the retinal, the protonation state of various groups, or the conformation of the protein. The study of these intermediates has provided much information about the proton transfer steps that make up the trajectory of the transported proton across the membrane. However, the central question in this system, as in any ion pump, is the nature of the internal step that separates the release of a proton at one surface from the uptake at the other. In bacteriorhodopsin this corresponds to the change in the connectivity of the retinal Schiff base (Nagle & Mille, 1981; Kalisky et al., 1981; Fodor et al., 1988a). Initially, it is to D85 with access to the extracellular surface, and later in the photocycle it is to D96 with access to the cytoplasmic surface. Thus, according to a proposed model (Váró & Lanyi, 1991b), the access of the Schiff base will change (in the $M_1 \rightarrow M_2$ step) after a proton is transferred from the Schiff base to the anionic D85 (the $L \rightarrow M_1$ step) but before a proton is transferred from the initially protonated D96 to the Schiff base (the $M_2 \rightarrow N$ step). This "reprotonation switch" has been associated (Kataoka et al., 1994) with a protein conformation change detected by diffraction (Koch et al., 1991; Nakasako et al., 1991; Subramaniam et al., 1993). The structural change occurs during the lifetime of the M state, and although its rise has not been possible to follow, it appears to decay with the N state (Koch et al., 1991). As measured with electron diffraction (Subramaniam et al., 1993), the most prominent

† This work was partly funded by a grant from the the National Institutes of Health (GM 29498). The high pressure device was purchased with funds from the 1994 Athalie Clark Research Award to J.K.L.

* Author to whom correspondence should be addressed.

‡ Permanent address: Institute of Biophysics, Biological Research Center of the Hungarian Academy of Sciences, H-6701 Szeged, Hungary.

⊗ Abstract published in *Advance ACS Abstracts,* September 1, 1995.

[1] Abbreviations: BR, K, L, M, N, and O refer to the unphotolyzed bacteriorhodopsin and intermediates of the photocycle. In M_1 and M_2 the retinal Schiff base is unprotonated and suggested to be connected to D85 and D96, respectively (*e.g.*, Lanyi, 1993). $N^{(-1)}$ and $N^{(0)}$ are substates of the N intermediate before and after proton uptake at the cytoplasmic surface (Zimányi et al., 1993).

0006-2960/95/0434-12161$09.00/0

feature of the structural change is the tilt of the cytoplasmic end of helix F away from the center of the protein. Besides its proposed effect on the access of the Schiff base, the conformational change could affect also the M → N protonation reaction in the cytoplasmic domain. Thus, it is possible that the more open structure at the cytoplasmic surface in the M conformation might cause increased hydration of the cytoplasmic domain and facilitate transfer of a proton from D96 to the Schiff base, as proposed from the inhibition of the forward and back-reactions of the M ⇔ N equilibrium at lowered water activity (Cao et al., 1991). A more precise description of the structural change would decide if this is a reasonable mechanism. Conformational changes in bacteriorhodopsin have been measured by other methods. However, the relationship of the changes detected by amide bands in FTIR spectra (Rothschild et al., 1981; Marrero & Rothschild, 1987; Ormos, 1991; Braiman et al., 1991; Sasaki et al., 1992; Perkins et al., 1992), and by spin labels linked to a residue at the cytoplasmic end of helix C (Steinhoff et al., 1994), to the diffraction changes in M is not yet clear.

A clue to the driving force for the conformational shift and the internal access change was provided by the finding that very similar diffraction changes occur in the dark when the Schiff base of the D85N mutant becomes deprotonated in the dark simply upon raising the pH (Kataoka et al., 1994). As in the photocycle of the wild type protein in M_2, the access of the Schiff base proton under these conditions is to the cytoplasmic side. The results suggested that the direct cause of the conformation change is the loss of the Schiff base−counterion interaction upon deprotonation of the Schiff base and confirmed the link betwen the conformational shift to the change of the internal proton transfer pathways.

A large-scale conformational change, such as observed in the M state of bacteriorhodopsin, can be expected to result in a volume change. Volume changes in proteins have two possible origins [reviewed, for example, in Heremans (1982) and Gross & Jaenicke (1994)]: (1) Since the location of many residues in the interior of proteins is determined by their tendency to participate in hydrogen bonding where possible, the average packing is not necessarily as compact as the closest approaches would produce. There is, therefore, a possibility for assuming more or less dense conformations, *i.e.*, smaller or larger overall volumes. (2) Since liquid water has a smaller volume than crystalline water, increased or decreased binding of water in different protein conformations will result in an increase or decrease in the total volume, respectively. The magnitude of volume changes during reactions can be determined either directly with photoacoustic measurements [reviewed in Peters et al. (1991)] or indirectly through the effect of pressure on the rate constants of reactions or equilibria. Pressure dependencies have been determined for light/dark adaptation of bacteriorhodopsin (Tsuda & Ebrey, 1980; Kovács et al., 1993; Schulte et al., 1995) and for the rate of the decay of the M intermediate (Tsuda et al., 1983; Marque & Eisenstein, 1984). We had expected that closer examination of the pressure dependencies of the photocycle reactions would reveal a significant volume increase between M_1 and M_2 that corresponds to the structural change found in M. This was indeed observed, as we report here. Additionally, we found a large positive activation volume for the proton exchange between the Schiff base and D96, described by the $M_2 \leftrightarrow N$ equilibrium. It is consistent with the increase of the free energy of the transition state in the presence of osmotic agents (Cao et al., 1991) that had suggested that the dipole environment provided by hydration of the cytoplasmic region is necessary for transferring a proton between D96 and the Schiff base. As expected from this, unlike in the wild type, the decay of the M intermediate of the D96N mutant is not inhibited by either high hydrostatic or osmotic pressure.

MATERIALS AND METHODS

Transient spectroscopy with a gated optical multichannel analyzer (Zimányi et al., 1989) and at single wavelengths (Cao et al., 1993) was as described before. Absorbance changes at varying hydrostatic pressures were determined in a pressure cell with three windows, two for the entry and exit of the measuring light and the third for the actinic laser flash, from ISS (Champaign, IL). The samples were thermostated at 20 °C. Acetate and CAPS were not ideal buffers at high pressures, but at 1 kbar their pK_a's changed by less than 0.1 pH units (Neuman et al., 1973). Calculations of the spectra of the photointermediates from time-resolved difference spectra was with the SEARCH program, written by L. Zimányi (Zimányi & Lanyi, 1993). Fits of kinetic models to the time courses of absorbance changes at single wavelengths and the calculated extinctions were with the RATE program, written by G. Groma. This program performs a global fit of a given model to the data. It allowed also the calculation of the time-dependent concentrations of the intermediates from the rate constants of the best fits.

RESULTS

Pressure Dependencies in the Photocycle of D96N Bacteriorhodopsin. Upon replacement of D96 with a nonprotonatable residue the photocycle is simplified because reprotonation of the Schiff base (M decay) is so slow that the N and O intermediates do not accumulate (Holz et al., 1989; Tittor et al., 1989; Otto et al., 1989; Miller & Oesterhelt, 1990; Cao et al., 1991). Further, this system at pH below 6 (the pK_a for proton release to the extracellular surface) is best suited for following the equilibrium in the M_1 to M_2 conversion because proton release at the $M_1 \rightarrow M_2$ reaction does not occur and for this reason the $M_2 \rightarrow M_1$ back-reaction becomes fast enough to be measurable (Zimányi et al., 1992b). Finally, in D96N M_1 and M_2 have different absorption maxima (Zimányi et al., 1992a) and can be distinguished by this property as well as kinetic analysis. We had described this photocycle under these conditions with the following equation:

$$BR \xrightarrow{h\nu} K \leftrightarrow L \leftrightarrow M_1 \leftrightarrow M_2 \rightarrow BR$$

Figure 1A shows that, as found before (Tsuda & Ebrey, 1980; Kovács et al., 1993), the main absorption band of the unphotolyzed chromophore in D96N shifts to somewhat longer wavelengths, and its amplitude increases at increased hydrostatic pressures. The spectra of the intermediates of the D96N photocycle at pH 5 were calculated from a multidimensional search for the best K, L, and M spectra from time-resolved difference spectra measured at 100 ns, 10 μs, and 4 ms, as described before (Zimányi & Lanyi, 1993). In this calculation the difference of the maxima of the two M states, which were 411 nm for M_1 and 406 nm

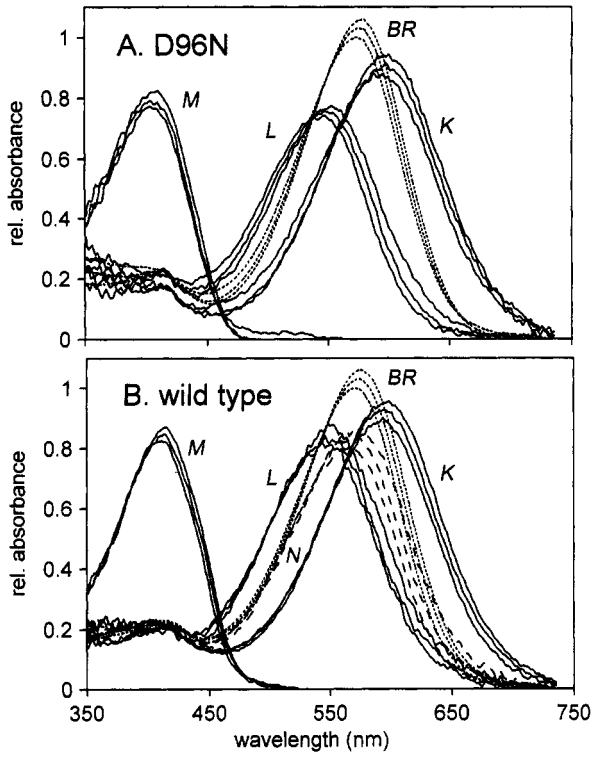

FIGURE 1: Spectra of the unphotolyzed D96N (A) and wild-type (B) bacteriorhodopsin and its photointermediates at various hydrostatic pressures. In all cases spectra are shown for 1 bar, 0.5 kbar, and 1 kbar, and they shift toward longer wavelength and increased amplitude at higher pressures. The spectra for the unphotolyzed chromophores were measured directly; for the intermediates they were calculated from time-resolved difference spectra as before (Zimányi & Lanyi, 1993). Conditions: for A, 100 mM NaCl, 5 mM sodium acetate, pH 5.0; for B, 100 mM NaCl, 50 mM CAPS, pH 10.0.

for M_2 (Zimányi et al., 1992a), was ignored. The results demonstrate that pressure affects the spectra of the intermediates much as that of the unphotolyzed state (Figure 1A).

The kinetics of absorbance changes were determined at 400, 411, 500, 570, and 640 nm, at various hydrostatic pressures between 1 bar and 1 kbar. In the traces for 411, 500, 570, and 640 nm, given in Figures 2 and 3, pressure-dependent shifts in the time constants and amplitudes of the changes are both evident. Because the pressure-dependence of the $M_1 \rightleftharpoons M_2$ equilibrium is of special interest, we paid particular attention to any differences at 400 and 411 nm as the pressure was increased. Figure 4 shows that at 1 bar the absorbance increase at 411 nm is initially (*e.g.*, between 1 and 10 μs) greater than the increase at 400 nm, indicating that the M substate that absorbs at the longer wavelength, *i.e.*, M_1, dominates, but the difference disappears between 1 and 10 ms because M_1 decays into M_2 with a maximum at shorter wavelength. However, at higher pressures the absorbance changes at 400 nm remain lower than those at 411 nm well into the ms time range, suggesting that M_1 persists increasingly at higher pressures.

The extinctions of K, L, M_1, and M_2 at the five wavelengths of the measurements were taken from the calculated spectra in Figure 1A, with small changes of the M spectrum made for M_1 and M_2, based on an earlier calculation of their spectra in D96N at pH 10, where as in the wild type (see below), M_1 accumulates in much greater amounts than at pH 5 and its contribution could be directly evaluated

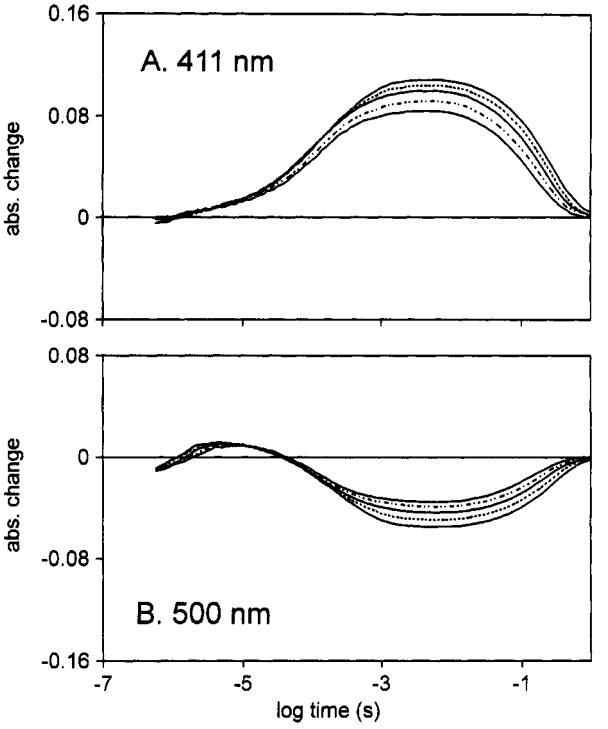

FIGURE 2: Absorbance changes at 411 (A) and 500 (B) nm after photoexcitation of D96N bacteriorhodopsin at various hydrostatic pressures. Lines: —, 1 bar; ···, 0.25 kbar; – –, 0.5 kbar; —·—, 0.75 kbar; and —, 1 kbar. Conditions as in Figure 1A.

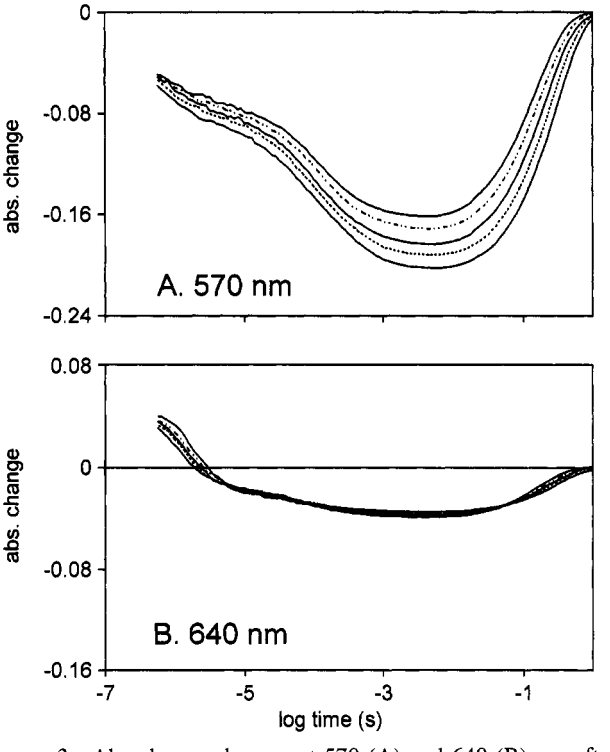

FIGURE 3: Absorbance changes at 570 (A) and 640 (B) nm after photoexcitation of D96N bacteriorhodopsin at various hydrostatic pressures. Lines: —, 1 bar; ···, 0.25 kbar; – –, 0.5 kbar; —·—, 0.75 kbar; and —, 1 kbar. Conditions as in Figure 1A.

(Zimányi et al., 1992a). From the time-courses and the extinctions we calculated the best fit of the kinetic scheme and the rate constants (see Materials and Methods). Measured traces at 411, 500, and 570 nm (solid lines) and the predictions of the model (dotted lines) are shown together in Figure 5A and B, for 1 bar and 1 kbar, respectively. The

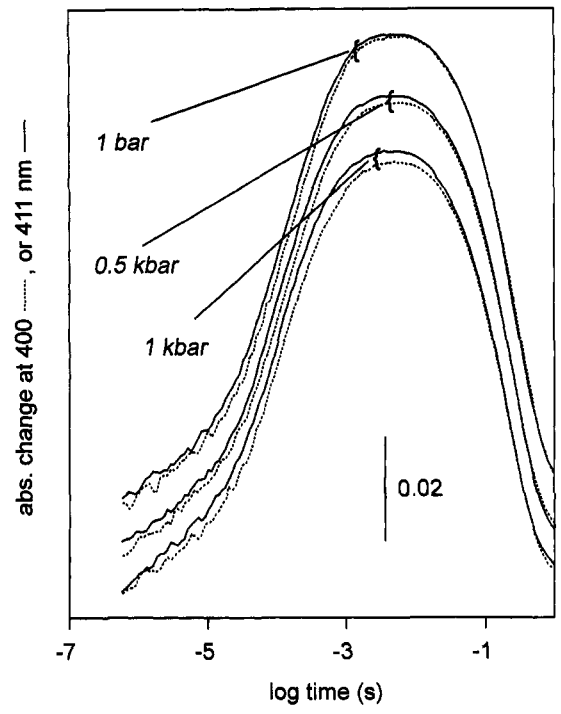

FIGURE 4: Absorbance changes at 400 and 411 nm after photoexcitation of D96N bacteriorhodopsin at three pressures. The three pairs of traces, at 1 bar, 0.5 kbar, and 1 kbar, as labeled, have been vertically displaced for clarity. The differences in the amplitudes at the two wavelengths suggest progressive shift in the ratio of M_1 and M_2 at the higher pressures toward M_1. Conditions as in Figure 1A.

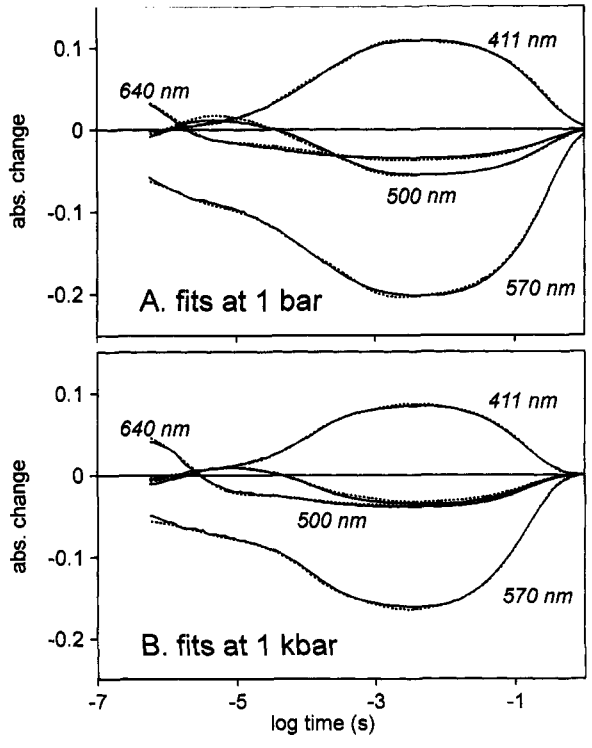

FIGURE 5: Measured absorbance changes in D96N bacteriorhodopsin, and the predictions of the best fit of the model, BR $\rightarrow(h\nu)$ K $\leftrightarrow$ L $\leftrightarrow$ M_1 $\leftrightarrow$ M_2 $\rightarrow$ BR. Although the global fits at 1 bar and 1 kbar were obtained from data at 400, 411, 500, 570, and 640 nm, only the last four are shown: solid lines, measurements; dotted lines, model. Conditions as in Figure 1A.

fits were reasonably good and had χ^2 values between 1.7×10^{-3} and 2.3×10^{-3}. The time-dependent concentrations

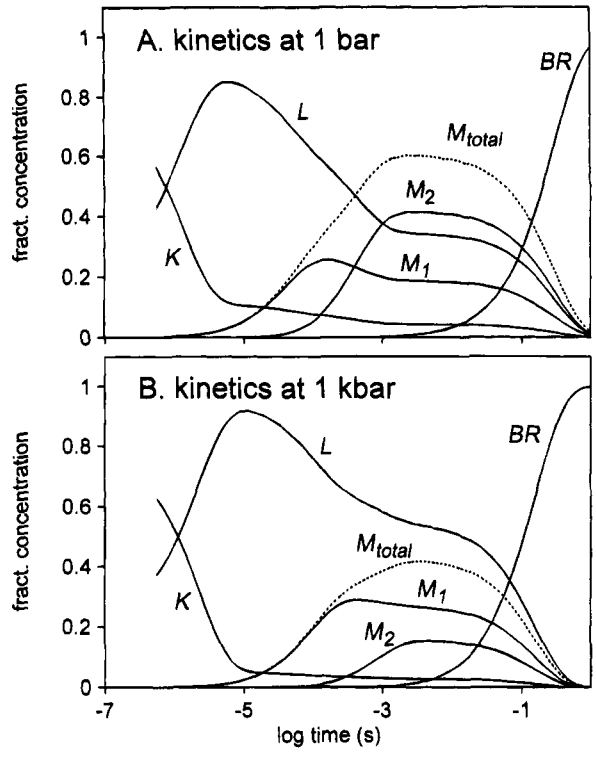

FIGURE 6: Calculated kinetics for the D96N bacteriorhodopsin photocycle from the rate constants of the best fits, at 1 bar (A) and 1 kbar (B). The concentrations of K, L, M_1, M_2, M_{total} (dotted line), and BR are given as fractions of the bacteriorhodopsin that entered the photocycle.

of K, L, M_1 and M_2 (and M_{total}, dotted lines) after photoexcitation at 1 bar and 1 kbar, calculated from the rate constants of the best fits, are shown in Figure 6A and B. At 1 bar decay of K leads to an equilibrium mixture of K and L, decay of L leads to an equilibrium that contains K, L, and M_1, and the further progress of the reaction produces an equilibrium that contains K, L, M_1, and M_2, as found earlier at pH < 6 in this mutant (Zimányi et al., 1992b). The most obvious change between 1 bar and 1 kbar is in the relative concentrations of the three states in the last equilibrium. At 1 kbar its composition is shifted away from M_2 and contains more L and M_1 than at the lower pressure. As a result of the increased persistence of L, the total amount of the M states that accumulates is lower.

The pressure dependence of rate constants is usually interpreted in terms of activation volumes, $\Delta V^{\ddagger}$, which refer to a volume change in the transition state. The activation volume is calculated from the pressure dependence at constant temperature from the following relationship (Gross & Jaenicke, 1994)

$$\ln k = \text{constant} - \frac{P\Delta V^{\ddagger}}{RT} \qquad (1)$$

where k is the rate constant of the given reaction, P is the hydrostatic pressure, R is the gas constant, and T is the absolute temperature. Figure 7 shows the logarithm of the rate constants of the D96N photocycle *vs* the pressure. In all cases the relationship is strictly linear, with negative slopes (positive activation volumes) for all reactions except the decay of the M state. The calculated activation volumes are given in Table 1.

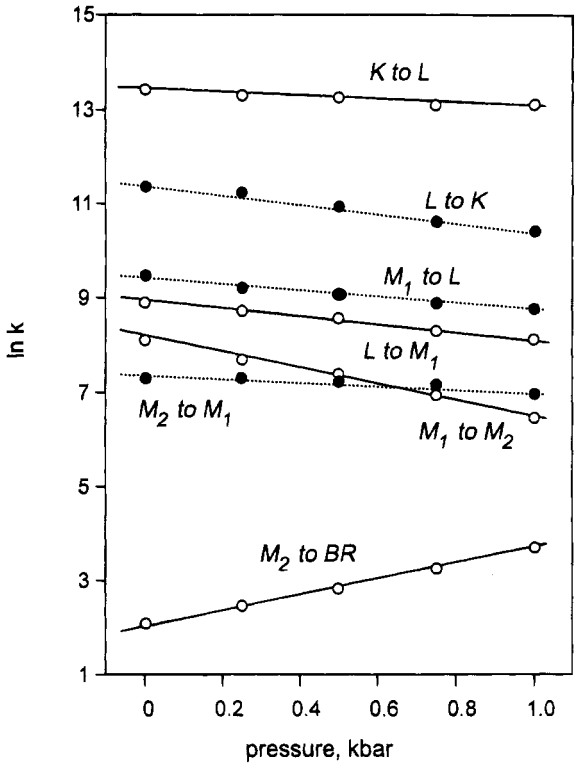

FIGURE 7: Dependence of the rate constants of the D96N bacteriorhodopsin photocycle on hydrostatic pressure. The rate constants were calculated by global fits of the model (see legend to Figure 5) to the data in Figures 2 and 3: open circles and solid lines, forward reactions; closed circles and dotted lines, back-reactions.

Table 1: Activation Volumes for the Photocycle Reactions of D96N and Wild-Type Bacteriorhodopsin, As Calculated from Their Dependence on Hydrostatic Pressure[a]

D96N		wild type	
reaction	$\Delta V^{\ddagger}$, mL/mol	reaction	$\Delta V^{\ddagger}$, mL/mol
K → L	8.3 ± 0.4	K → L	6.8 ± 0.3
L → K	24.1 ± 1.0	L → K	25.6 ± 0.7
L → M_1	19.2 ± 0.8	L → M_1	13.1 ± 0.5
M_1 → L	16.8 ± 0.5	M_1 → L	8.8 ± 0.5
M_1 → M_2	39.4 ± 1.2	M_1 → M_2	18.5 ± 0.6
M_2 → M_1	7.7 ± 0.9	M_2 → $N^{(-1)}$	50.1 ± 1.5
M_2 → BR	−39.2 ± 1.1	$N^{(-1)}$ → M_2	44.8 ± 2.1
		$N^{(-1)}$ → $N^{(0)}$	15.6 ± 0.6
		$N^{(0)}$ → $N^{(-1)}$	7.1 ± 1.6
		$N^{(0)}$ → BR	0.6 ± 0.3

[a] The activation volumes are from the slopes of the curves, and their standard deviations, in Figures 7 and 12.

Pressure Dependencies in the Photocycle of Wild-Type Bacteriorhodopsin. At pH > 8.5 in the wild-type photocycle the decay of M deviates prominently from a single exponential. We, as others (Otto et al., 1989; Gerwert et al., 1990; Souvignier & Gerwert, 1992; Ames & Mathies, 1990; Váró & Lanyi, 1990, 1991a; Cao et al., 1991; Druckmann et al., 1993; Zimányi et al., 1993), have interpreted a large amount of data on this phenomenon as the equilibration of M with N followed by the slower decay of N. This behavior appears only at high pH because the decay of N is linked to proton uptake at the cytoplasmic surface, and evidently at pH > 8.5 protons begin to limit its rate. The O intermediate does not accumulate under these conditions. Closer examination of the kinetics had revealed (Zimányi et al., 1993) that proton uptake occurs in fact during the lifetime of N, and two N substates exist, $N^{(-1)}$ before proton uptake and $N^{(0)}$ after, as

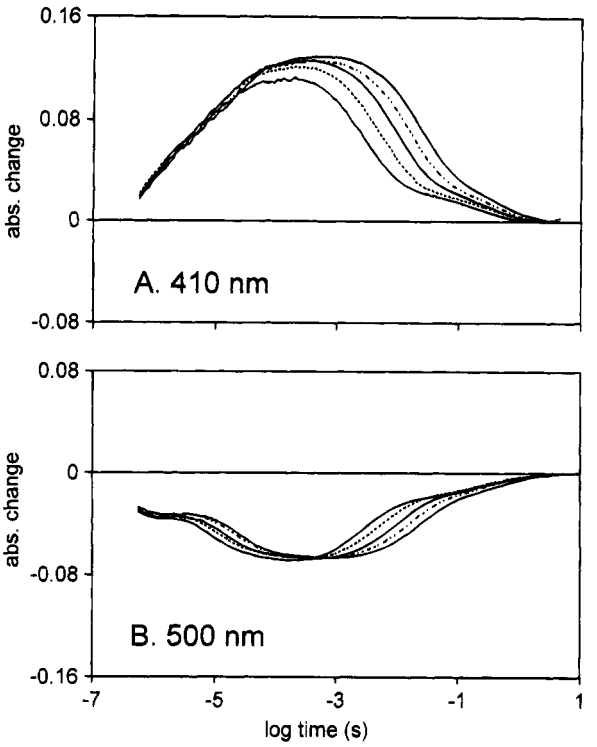

FIGURE 8: Absorbance changes at 410 (A) and 500 (B) nm after photoexcitation of wild type bacteriorhodopsin at various hydrostatic pressures. Lines: —, 1 bar; ▪, 0.25 kbar; —, 0.5 kbar; —▪—, 0.75 kbar; and —, 1 kbar. Conditions as in Figure 1B.

predicted earlier (Fodor et al., 1988a). Since the apparent pK_a for the proton uptake is about 11 (Zimányi et al., 1993), at sufficiently high pH all reactions between M_2 and $N^{(0)}$ in this scheme are reversible, and their activation volumes should yield also the relative volumes of the intermediates. On the other hand, since under these conditions the $N^{(-1)} + H^+ \rightarrow N^{(0)}$ reaction is limited by proton concentration rather than what occurs in the protein that triggers the proton uptake, the pressure dependence of this reaction might not be relevant to a possible protein volume change at this step.

The spectra of the unphotolyzed wild type protein, and the spectra of the K, L, M, and N intermediates of the photocycle at pH 10, were determined at various pressures from time-resolved difference spectra at 100 ns, 4 μs, 100 μs, and 10 ms, in the same way as for D96N in Figure 1A. The resulting spectra are shown in Figure 1B. The spectra of BR, K, L, and M, and their pressure dependencies, are very similar to those in D96N, and the spectrum of N also follows the trend of red-shift and increased amplitude at higher pressure.

Figures 8 and 9 show absorbance changes after photoexcitation, measured at 410, 500, 570, and 640 nm and 1, 250, 500, 750, and 1000 bar. As in the data for D96N, there are progressive changes with pressure at all wavelengths, but the changes are different. For example, the amplitude of the absorbance rise at 410 nm increases rather than decreases with pressure, and a substantial slowing of the M decay rather than acceleration is seen. In contrast with the traces for D96N, the maximal amplitude at 500 nm is hardly changed but at 640 nm considerably increased (compare Figures 2 and 3 with Figures 8 and 9). The sequential model (Zimányi et al., 1993)

$$BR \xrightarrow{h\nu} K \leftrightarrow L \leftrightarrow M_1 \rightarrow M_2 \leftrightarrow N^{(-1)} \leftrightarrow N^{(0)} \rightarrow BR$$

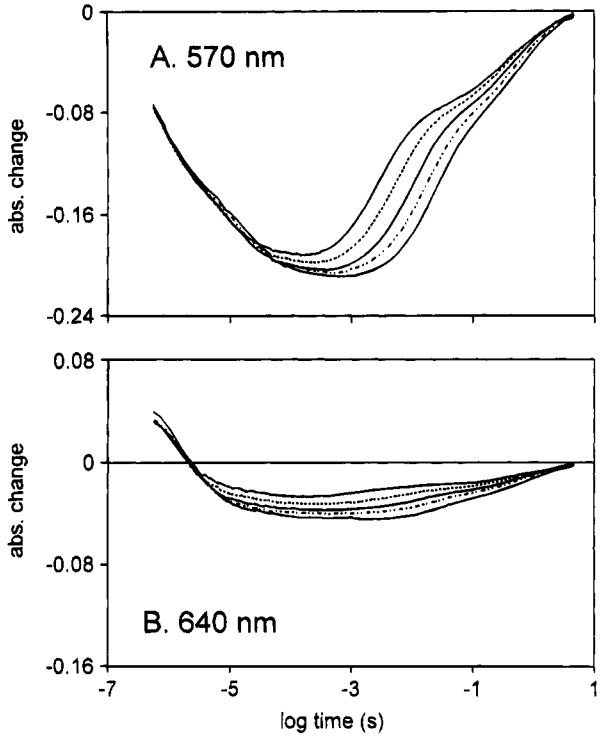

FIGURE 9: Absorbance changes at 570 (A) and 640 (B) nm after photoexcitation of wild-type bacteriorhodopsin at various hydrostatic pressures. Lines: —, 1 bar; ···, 0.25 kbar; – –, 0.5 kbar; —·—, 0.75 kbar; and —, 1 kbar. Conditions as in Figure 1B.

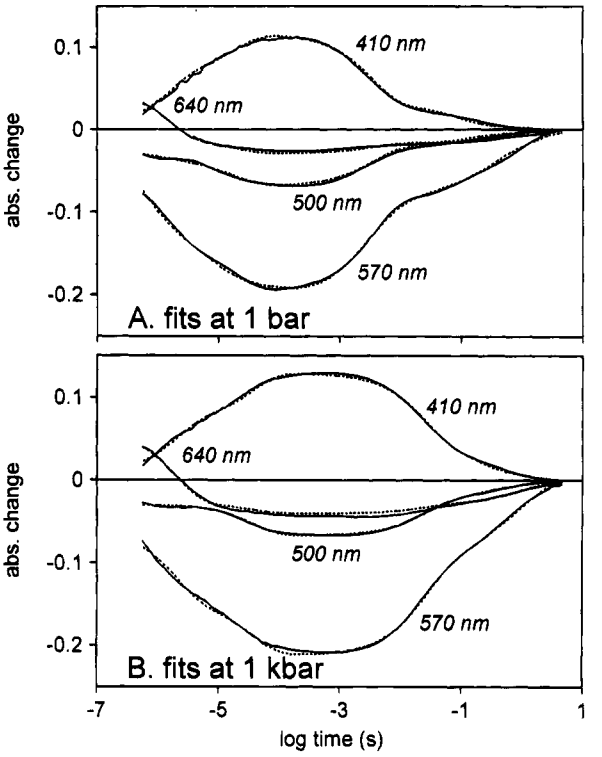

FIGURE 10: Measured absorbance changes in wild-type bacteriorhodopsin, and the predictions of the best fit of the model, BR $\rightarrow(h\nu)$ K $\leftrightarrows$ L $\leftrightarrows$ M_1 $\leftrightarrows$ M_2 $\leftrightarrows$ $N^{(-1)}$ $\leftrightarrows$ $N^{(0)}$ $\rightarrow$ BR. The global fits at 1 bar and 1 kbar were obtained from data at 410, 500, 570, and 640 nm, as shown: solid lines, measurements; dotted lines, model. Conditions as in Figure 1B.

was fitted to these traces, except that the $M_2 \rightarrow M_1$ back-reaction was allowed as a test. In the best fits the rate of this reaction was negligible at all pressures, consistent with the previous finding (Váró & Lanyi, 1991a) that at pH > 7 the $M_1 \rightarrow M_2$ is essentially irreversible. The predictions of the best fits together with the data at 1 bar and 1 kbar are shown in Figure 10A and B, respectively. The χ^2 values were between 1.7×10^{-3} and 2.7×10^{-3}. The calculated kinetics at 1 bar and 1 kbar are in Figure 11A and B. At 1 bar the complete decay of the equilibrium mixture that contains K, L, and M_1, with the production of M_2, is evident, as well as the equilibration of M_2 with first $N^{(-1)}$ and then also with $N^{(0)}$. The second decay component of M, which corresponds to the $M_2 \leftrightarrows N^{(-1)}$ equilibrium, is prominent, and at this high pH the third component that gave rise to the proposal of the $M_2 \leftrightarrows N^{(-1)} \leftrightarrows N^{(0)}$ equilibrium (Zimányi et al., 1993) is also evident. The most obvious changes with pressure are in the decay of M_2. Although their formation is slowed, and their amplitudes are somewhat less, the ratio of the accumulated $N^{(-1)}$ and $N^{(0)}$ is not very different at the higher pressure.

The pressure dependencies of the rate constants are shown in Figure 12 and the calculated activation volumes in Table 1. The more rapid rise of the M state at the high pH (Balashov et al., 1991) originates in this model from greatly increased rate constants in the L $\leftrightarrows$ M_1 equilibrium. This is not a difference between the mutant and the wild type, because the kinetics up to M are only slightly different in the wild type and D96N when measured at the same pH (Thorgeirsson et al., 1991; Zimányi et al., 1993). Toward the end of the photocycle, the $N^{(-1)} \rightarrow N^{(0)}$ reaction is more rapid than its back-reaction, but the latter is not negligible so near the pK_a for the uptake as it is at lower pH. Up to M_1, the activation volumes are similar to those of D96N, but the $\Delta V^{\ddagger}$ for the $M_1 \rightarrow M_2$ reaction is substantially less than in D96N. The largest activation volumes are for the forward and back-reactions in the $M_2 \leftrightarrows N^{(-1)}$ equilibrium, and there is no negative volume of activation. The recovery of the initial state is essentially pressure independent, unlike in D96N where it has a large negative activation volume.

DISCUSSION

We have examined the way hydrostatic pressure affects the individual reactions of the bacteriorhodopsin photocycle, with the intention of identifying the steps in which conformational changes cause volume increase or decrease. Specifically, we tested the hypothesis that a helical tilt at the cytoplasmic surface (Subramaniam et al., 1993), which would expose the interhelical region to increased hydration and thereby increase the volume, is associated with the access change for the Schiff base proton, the "reprotonation switch," detected as the $M_1 \rightarrow M_2$ step in the photocycle (Kataoka et al., 1994). Establishing the difference between the volumes of M_1 and M_2 required conditions where both the $M_1 \rightarrow M_2$ forward reaction and the $M_2 \rightarrow M_1$ back-reaction are unambiguously measured. This could be accomplished in the D96N mutant at pH 5, where as reported before (Zimányi et al., 1992b), the reaction is reversible and the two substates of M are distinguishable by their different absorption maxima. However, in this mutant the M_2 state decayed so slowly that none of the intermediates between M_2 and BR accumulated. Kinetic separation of the decay of M from the decay of N in the wild-type protein, which allows measurement of the M $\leftrightarrows$ N equilibrium, occurs only at high pH, *i.e.*, pH 10. Since the proton uptake is slow under these

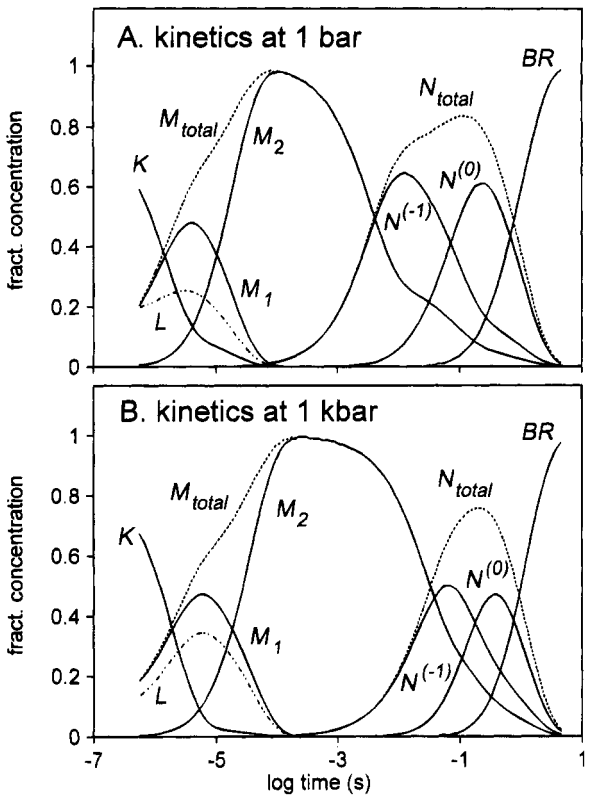

FIGURE 11: Calculated kinetics for the wild-type photocycle from the rate constants of the best fits, at 1 bar (A) and 1 kbar (B). The concentrations of K, L, M_1, M_2, M_{total} (dotted line), $N^{(-1)}$, $N^{(0)}$, N_{total} (dotted line), and BR are given as fractions of the bacteriorhodopsin that entered the photocycle.

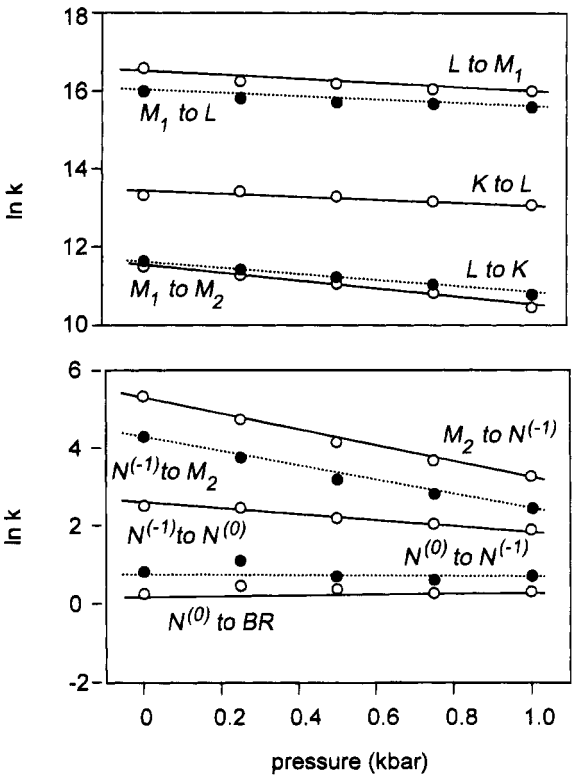

FIGURE 12: Dependence of the rate constants of the wild-type bacteriorhodopsin photocycle on hydrostatic pressure. The rate constants were calculated by global fits of the model (see legend to Figure 10) to the data in Figures 8 and 9: open circles and solid lines, forward reactions; closed circles and dotted lines, back-reactions.

conditions, the internal proton equilibration between D96 and the Schiff base (the $M_2 \Leftrightarrow N^{(-1)}$ reaction) is well separated in time from the proton uptake (the $N^{(-1)} + H^+ \rightarrow N^{(0)}$ reaction) and the recovery of the initial state (the $N^{(0)} \rightarrow BR$ reaction). However, under these conditions the proton uptake is limited by proton concentration (Zimányi et al., 1993), and a volume change in $N^{(0)}$ as revealed by the effects by hydrostatic pressure would be obscured. As a result, we could identify the location of the volume increase in the photocycle as the $M_1 \rightarrow M_2$ reaction, but were only able restrict its reversal to the decay of either $N^{(-1)}$ or $N^{(0)}$, without identifying it more exactly.

The activation volumes and volume changes up to M_1 in the wild type and D96N are graphically represented in Figure 13. Between K and M_1 the changes are similar in the two proteins. There is some volume decrease between K and L, which might be related to the relaxation of the strained 13-*cis* retinal in the binding pocket (Diller & Stockburger, 1988; Fodor et al., 1988b) or to the rearrangement of water bound near the Schiff base (Maeda et al., 1992, 1994; Kandori et al., 1995). The L to M_1 reaction results in a small volume increase. In D96N we observe an approximately 32 mL/mol volume increase between M_1 and M_2 (Figure 13A). It is because of this volume increase that the forward $M_1 \rightarrow M_2$ reaction is inhibited by increasing pressure but the reverse reaction is hardly affected (Figure 7). The relative contributions of changed residue packing and increased water binding to this volume increase are uncertain. If the volume change had originated entirely from increased water binding, and the ΔV/mol for bound water can be estimated from the liquid water to ice transition, the increase of volume between M_1 and M_2 would be equivalent to the binding of about 20 water molecules. Assuming that the volumes of the unphotolyzed state and the K intermediate are roughly the same (Schulenberg et al., 1994), the net volume increase in the M_2 intermediate is about 20 mL/mol. This is roughly what would be expected[2] from the change of the surface area as calculated from the increase of the lattice constant in M (Nakasako et al., 1991). We conclude that the pressure dependence at the $M_1 \rightarrow M_2$ reaction detects a conformation change of about the same magnitude as predicted by the changed diffraction of the M state and might originate mainly from water binding.

Since the volume changes are given by the differences between the activation volumes of the forward and the reverse reactions, and the $M_1 \rightarrow M_2$ reaction is unidirectional at pH 10 (Váró & Lanyi, 1991a; Zimányi et al., 1992a,b), the relative volumes of M_1 and M_2 could not be measured in the experiments with wild-type protein. Importantly, however, nowhere in the photocycle under these conditions was there a volume increase comparable to 32 mL/mol (Figure 13B). Given that the diffraction changes were found to be similar in the M states of the wild type and D96 mutant proteins (Subramaniam et al., 1993), the changed M conformation will have been assumed during the photocycle of

[2] From the lattice constant in the M (*i.e.*, M_2) state, relative to the unphotolyzed protein in the purple membrane, we calculate that if the cross-sectional increase is caused entirely by increase of the area of the cytoplasmic surface, its increase is by 36 Å^2/unit cell in projection. This yields 12 Å^2/bacteriorhodopsin. Depending on the depth of the cleft that develops in the M_2 state, such an increase would accommodate perhaps 10−20 water molecules.

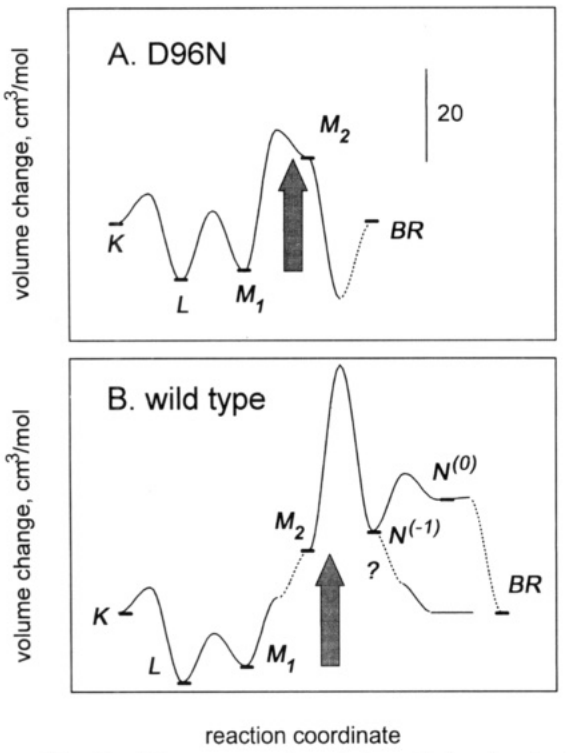

FIGURE 13: Graphic representation of the calculated activation volumes and volume changes in the photocycles of D96N bacteriorhodopsin (A) and wild-type bacteriorhodopsin (B). The vertical calibration bar applies to both A and B. The solid lines show the changes calculated directly from the pressure dependencies. The dotted lines indicate changes for which direct measurements are not available. The shaded arrows indicate the largest volume change in the photocycle, which we believe corresponds to the protein conformation change detected by diffraction (cf. text). We assumed that the volume of K is not much different from the unphotolyzed state. In the wild type we have drawn the volume of M_2 relative to the volume of M_1 as in D96N. Since the $N^{(-1)} + H^+ \rightarrow N^{(0)}$ reaction in the wild type is limited by proton concentration, the activation volume at this step might not originate from a conformation change occuring in the protein. For this reason we have drawn in, with a question mark, a second alternative for the recovery of the volume increase at this reaction.

both proteins. If the volume increase we detect in D96N corresponds to this change, and there is a volume increase also in the wild type, it must occur in the $M_1 \rightarrow M_2$ reaction as in the mutant. However, perhaps related to the much reduced energy barrier to the proton exchange between the Schiff base and D85 at pH 10 (Figure 12), the activation volume is lower than in D96N.

The reversal of the volume increase is more ambiguous. According to the pressure dependencies of the rates, M_2, $N^{(-1)}$ and $N^{(0)}$ have roughly the same volumes. However, under the conditions of the measurement the rate of the $N^{(-1)} + H^+ \rightarrow N^{(0)}$ reaction is limited by proton concentration, and its small pressure dependence (Figure 12) will have originated from the activation volume of the proton uptake process, rather than any changes of the protein. In the T46V mutant, the decay of M and N are similarly separated in time, but the N that accumulates is $N^{(-1)}$ and its decay is not limited by pH (Brown et al., 1994). In the protein the decay of N is accelerated rather than slowed at high hydrostatic pressure.[3] Although pH dependent, the decay of M in D96N is greatly slowed by what appears to be a large entropic barrier to proton uptake (Cao et al., 1991), and it also has a negative activation volume (Table 1, Figure 13A). It is possible, therefore, that the initial lower volume is recovered already in $N^{(0)}$, rather than during the decay of $N^{(0)}$ as might be surmised from the results in Figure 13B. Either case would be consistent with the earlier suggestion, made from the pH dependence of the decay of the diffraction change, that the conformational state relaxes together with N (Koch et al., 1991). We suggest that the results with D96N and the wild type agree with one another and with the diffraction changes and that the volume increase/diffraction change occurs in the $M_1 \rightarrow M_2$ reaction. It reverses as one of the two sequential N states decays, probably during the uptake of the proton at the cytoplasmic surface.

Photoacoustic measurements determine the volume changes of a reaction sequence in a model-independent way. Correspondence between volume increase or decrease found by this method and individual reactions must be established therefore on the basis of their time-constants. According to recent results with photoacoustic spectroscopy, the volume changes in the bacteriorhodopsin photocycle consist of a 60 mL/mol increase at 1.3 μs, followed by a 145 mL/mol increase at 90 μs, and a 185 mL/mol decrease at 6 ms (Schulenberg et al., 1995). The first increase corresponds to the K to L reaction, and we do not find its equivalent in the pressure dependencies. The second increase corresponds to the $M_1 \rightarrow M_2$ reaction, but like the decrease that follows, it is much larger than what we measure in the cycle. The cause of this discrepancy is not clear. Volume increases of this magnitude usually accompany complete unfolding of proteins (Gross & Jaenicke, 1994).

Although in principle the reactions of membrane enzymes could be affected by high hydrostatic pressures additionally through increased viscosity of the lipid bilayer (as discussed in Marque & Eisenstein, 1984), this is unlikely in the case of bacteriorhodopsin which is immobilized in the rigid 2-dimensional hexagonal structure of the purple membrane where the amount of lipid is just sufficient to form single annular layers in and around the protein lattice (Blaurock, 1975). Indeed, in most reports pressure effects in this system are interpreted in terms of volume changes. Nevertheless, we considered the possibility that what we observed does not reflect volume changes and in particular not volume changes from changed binding of water. If the pressure dependencies originated mostly, or entirely, from binding of water in the protein in the transition states and the intermediates of the photocycle, the same effects would be observed also with osmotic agents because they lower the water activity. Agreement of results obtained with increased hydrostatic pressure and lowered water activity would justify therefore the calculations of the activation volumes for the reactions, $\Delta V^{\ddagger}$, and the volume changes for successive intermediates, ΔV, from the pressure dependence, as we do here. The earlier found prominent and specific increase of the barrier in the $M \leftrightarrow N$ equilibrium by osmotic agents, such as sucrose (Cao et al., 1991), suggests that this step should be more sensitive to hydrostatic pressure than other reactions in the photocycle. The largest $\Delta V^{\ddagger}$ was indeed found in the $M \leftrightarrow N$ equilibrium, and for both forward and reverse reactions (Table 1, Figure 13B). What is the physical meaning of this large activation volume? In the earlier report we had attributed the main part of the barrier to the need for

[3] L. S. Brown, G. Váró, R. Needleman, & J. K. Lanyi, manuscript in preparation.

dipole stabilization of the transition state by water bound within the protein matrix, which would allow separation of the proton from the negatively charged carboxylic group of D96 (Cao et al., 1991). Indeed, as expected from this, the inhibitory effect of osmotic agents on the reprotonation of the Schiff base disappeared, and in fact reversed in the D96N mutant. This is true also for inhibition of this reaction by hydrostatic pressure (Table 1, Figure 13A). Thus, there is good correspondence between the conclusions drawn from the effects of osmotic and hydrostatic pressures on the reprotonation of the Schiff base, and it identifies the activation volume in the M ⇔ N equilibrium (Figure 13B) as the increasing hydration of the protein in the transition state.

ACKNOWLEDGMENT

The authors are very grateful to S. E. Braslavsky for making her paper available to them before its publication in *J. Phys. Chem.*

REFERENCES

Ames, J. B., & Mathies, R. A. (1990) *Biochemistry 29*, 7181−7190.
Balashov, S. P., Govindjee, R., & Ebrey, T. G. (1991) *Biophys. J. 60*, 475−490.
Blaurock, A. E. (1975) *J. Mol. Biol. 93*, 139−158.
Braiman, M. S., Bousché, O., & Rothschild, K. J. (1991) *Proc. Natl. Acad. Sci. U.S.A. 88*, 2388−2392.
Brown, L. S., Yamazaki, Y., Maeda, M., Sun, L., Needleman, R., & Lanyi, J. K. (1994) *J. Mol. Biol. 239*, 401−414.
Cao, Y., Váró, G., Chang, M., Ni, B., Needleman, R., & Lanyi, J. K. (1991) *Biochemistry 30*, 10972−10979.
Cao, Y., Váró, G., Klinger, A. L., Czajkowsky, D. M., Braiman, M. S., Needleman, R., & Lanyi, J. K. (1993) *Biochemistry 32*, 1981−1990.
Diller, R., & Stockburger, M. (1988) *Biochemistry 27*, 7641−7651.
Druckmann, S., Heyn, M. P., Lanyi, J. K., Ottolenghi, M., & Zimányi, L. (1993) *Biophys. J. 65*, 1231−1234.
Ebrey, T. G. (1993) In *Thermodynamics of membranes, receptors and channels*, (Jackson, M., Ed.) pp 353−387, CRC Press, New York.
Fodor, S. P., Ames, J. B., Gebhard, R., van der Berg, E. M., Stoeckenius, W., Lugtenburg, J., & Mathies, R. A. (1988a) *Biochemistry 27*, 7097−7101.
Fodor, S. P., Pollard, W. T., Gebhard, R., van den Berg, E. M., Lugtenburg, J., & Mathies, R. A. (1988b) *Proc. Natl. Acad. Sci. U.S.A. 85*, 2156−2160.
Gerwert, K., Souvignier, G., & Hess, B. (1990) *Proc. Natl. Acad. Sci. U.S.A. 87*, 9774−9778.
Gross, M., & Jaenicke, R. (1994) *Eur. J. Biochem. 221*, 617−630.
Holz, M., Drachev, L. A., Mogi, T., Otto, H., Kaulen, A. D., Heyn, M. P., Skulachev, V. P., & Khorana, H. G. (1989) *Proc. Natl. Acad. Sci. U.S.A. 86*, 2167−2171.
Heremans, K. (1982) *Annu. Rev. Biophys. Bioeng. 11*, 1−21.
Kalisky, O., Ottolenghi, M., Honig, B., & Korenstein, R. (1981) *Biochemistry 20*, 649−655.
Kandori, H., Yamazaki, Y., Sasaki, J., Needleman, R., Lanyi, J. K., & Maeda, A. (1995) *J. Am. Chem. Soc. 117*, 2118−2119.
Kataoka, M., Kamikubo, H., Tokunaga, F., Brown, L. S., Yamazaki, Y., Maeda, A., Sheves, M., Needleman, R., & Lanyi, J. K. (1994) *J. Mol. Biol. 243*, 621−638.
Koch, M. H. J., Dencher, N. A., Oesterhelt, D., Plöhn, H.-J., Rapp, G., & Büldt, G. (1991) *EMBO J. 10*, 521−526.
Kovács, I., Nienhaus, G. U., Philipp, R., & Xie, A. (1993) *Biophys. J. 64*, 1187−1193.
Krebs, M. P., & Gobind Khorana, H. (1993) *J. Bacteriol. 175*, 1555−1560.
Lanyi, J. K. (1993) *Biochim. Biophys. Acta Bio-Energetics 1183*, 241−261.
Lozier, R. H., Xie, A., Hofrichter, J., & Clore, G. M. (1992) *Proc. Natl. Acad. Sci. U.S.A. 89*, 3610−3614.
Maeda, A., Sasaki, J., Shichida, Y., & Yoshizawa, T. (1992) *Biochemistry 31*, 462−467.
Maeda, A., Sasaki, J., Yamazaki, Y., Needleman, R., & Lanyi, J. K. (1994) *Biochemistry 33*, 1713−1717.
Marque, J., & Eisenstein, L. (1984) *Biochemistry 23*, 5556−5563.
Marrero, H., & Rothschild, K. J. (1987) *Biophys. J. 52*, 629−635.
Mathies, R. A., Lin, S. W., Ames, J. B., & Pollard, W. T. (1991) *Annu. Rev. Biophys. Biophys. Chem. 20*, 491−518.
Miller, A., & Oesterhelt, D. (1990) *Biochim. Biophys. Acta Bio-Energetics 1020*, 57−64.
Nagle, J. F., & Mille, M. (1981) *J. Chem. Phys. 74*, 1367−1372.
Nakasako, M., Kataoka, M., Amemiya, Y., & Tokunaga, F. (1991) *FEBS Lett. 292*, 73−75.
Neuman, R. C., Jr., Kauzmann, W., & Zipp, A. (1973) *J. Phys. Chem. 77*, 2687−2691.
Ormos, P. (1991) *Proc. Natl. Acad. Sci. U.S.A. 88*, 473−477.
Otto, H., Marti, T., Holz, M., Mogi, T., Lindau, M., Khorana, H. G., & Heyn, M. P. (1989) *Proc. Natl. Acad. Sci. U.S.A. 86*, 9228−9232.
Perkins, G. A., Liu, E., Burkard, F., Berry, E. A., & Glaeser, R. M. (1992) *J. Struct. Biol. 109*, 142−151.
Peters, K. S., Watson, T., & Marr, K. (1991) *Annu. Rev. Biophys. Biophys. Chem. 20*, 343−362.
Rothschild, K. J., Zagaeski, M., & Cantore, W. A. (1981) *Biochem. Biophys. Res. Commun. 103*, 483−489.
Sasaki, J., Shichida, Y., Lanyi, J. K., & Maeda, A. (1992) *J. Biol. Chem. 267*, 20782−20786.
Schulenberg, P. J., Rohr, M., Gärtner, W., & Braslavsky, S. E. (1994) *Biophys. J. 66*, 838−843.
Schulenberg, P. J., Gärtner, W., & Braslavsky, S. E. (1995) *J. Phys. Chem. 99*, 9617−9624.
Schulte, A., Bradley, L, II, & Williams, C. (1995) *Appl. Spectrosc. 49*, 80−83.
Souvignier, G., & Gerwert, K. (1992) *Biophys. J. 63*, 1393−1405.
Steinhoff, H.-J., Mollaaghababa, R., Altenbach, C., Hideg, K., Krebs, M., Khorana, H. G., & Hubbell, W. L. (1994) *Science 266*, 105−107.
Subramaniam, S., Gerstein, M., Oesterhelt, D., & Henderson, R. (1993) *EMBO J. 12*, 1−8.
Thorgeirsson, T. E., Milder, S. J., Miercke, L. J. W., Betlach, M. C., Shand, R. F., Stroud, R. M., & Kliger, D. S. (1991) *Biochemistry 30*, 9133−9142.
Tittor, J. (1991) *Curr. Biol. 1*, 534−538.
Tittor, J., Soell, C., Oesterhelt, D., Butt, H.-J., & Bamberg, E. (1989) *EMBO J. 8*, 3477−3482.
Tsuda, M., & Ebrey, T. G. (1980) *Biophys. J. 30*, 149−157.
Tsuda, M., Govindjee, R., & Ebrey, T. G. (1983) *Biophys. J. 44*, 249−254.
Váró, G., & Lanyi, J. K. (1990) *Biochemistry 29*, 2241−2250.
Váró, G., & Lanyi, J. K. (1991a) *Biochemistry 30*, 5008−5015.
Váró, G., & Lanyi, J. K. (1991b) *Biochemistry 30*, 5016−5022.
Zimányi, L., & Lanyi, J. K. (1993) *Biophys. J. 64*, 240−251.
Zimányi, L., Keszthelyi, L., & Lanyi, J. K. (1989) *Biochemistry 28*, 5165−5172.
Zimányi, L., Cao, Y., Chang, M., Ni, B., Needleman, R., & Lanyi, J. K. (1992a) *Photochem. Photobiol. 56*, 1049−1055.
Zimányi, L., Váró, G., Chang, M., Ni, B., Needleman, R., & Lanyi, J. K. (1992b) *Biochemistry 31*, 8535−8543.
Zimányi, L., Cao, Y., Needleman, R., Ottolenghi, M., & Lanyi, J. K. (1993) *Biochemistry 32*, 7669−7678.

BI951290C